Polym. Bull. (2012) 69:105–123
DOI 10.1007/s00289-012-0742-x

ORIGINAL PAPER

Study on properties of simul wood (*Bombax ceiba* L.) impregnated with styrene acrylonitrile copolymer, TiO_2, and nanoclay

Rashmi R. Devi · Tarun K. Maji

Received: 10 November 2011 / Revised: 23 January 2012 / Accepted: 16 March 2012 /
Published online: 23 March 2012

Abstract Dimensional stability, thermal, and water repellency are very important properties of wood. In this research, wood polymer nanocomposite (WPNC) has been prepared by impregnation of styrene acrylonitrile copolymer (SAN), γ-trimethoxy silyl propyl methacrylate-modified TiO_2 nanoparticles, nanoclay into simul (*Bombex ceiba* L.) wood. The characterization of the composites was done by using Fourier transform infrared spectroscopy, X-ray diffractometry, and thermogravimetry. The resultant WPNC exhibited an improvement in water repellency, moisture resistance, dimensional stability, chemical resistance, hardness, and thermal stability. The maximum improvement in all the properties has been observed for the wood sample treated with SAN/TiO_2 (0.5 %)/nanoclay (0.5 %).

Keywords Impregnation · TiO_2 nanoparticles · Nanoclay · SAN · Wood · Mechanical properties

Introduction

Wood is a native material sensitive to humidity because of the hydrophilic nature of its cell wall constituent polymers cellulose, hemicelluloses, and lignin. As a result, the moisture content (MC) of wood varies with the proximate humidity and temperature changes. MC deviation below fiber saturation point causes dimensional changes in wood. Detrimental dimensional changes lead to cracking and twisting, shrinkage and swelling, and cause important practical problems in wood utilization for building and construction. In addition, excessive moisture can result in fungal

R. R. Devi · T. K. Maji (✉)
Department of Chemical Sciences, Tezpur University, Napaam, Tezpur 784028, Assam, India
e-mail: tkm@tezu.ernet.in

R. R. Devi
e-mail: rekha@tezu.ernet.in

attack leading to color changes and in the worst case—degradation. To achieve long-term service life, wood must have proper protection. The main reason for its hygroscopicity is that the wood fibers present a polar surface associated to the hydroxylated nature of the constituting anhydroglucose units. Such feature is responsible for the high hydrophilicity of wood, enabling the establishment of strong hydrogen bonding between fibers and the formation of three-dimensional wood [1].

Chemical modification is one of the means to counteract against the negative properties of wood. Over the decades the impregnation with polymers—leading to wood polymer composite (WPC) was intensively investigated [2–7]. WPCs have improved strength properties, elevated dimensional stability, and higher resistance to bio-deterioration. The preparation of WPCs by using thermoplastic polymer and lignocellulosic filler from non-wood plant materials has been reported in the literature [8–10].

Nano-based treatments put forward innovative opportunities boosting wood attributes more efficiently for diverse applications in the horizon of wood modification processes. The preparation of wood polymer nanocomposites (WPNCs) based on impregnation of water soluble thermosetting polymer and clay and study on its physical, mechanical properties enhancement has been found in the literature [11, 12]. Water repellency, dimensional stability, mechanical, and thermal properties of wood polymer/clay nanocomposite prepared by vacuum impregnation of styrene acrylonitrile copolymer (SAN) and nanoclay was also investigated in our previous studies [13, 14]. Nourbakhsh et al. [15] has studied the different physico-mechanical properties of fiber reinforced composites (FRC) prepared by using polypropylene and hybrid fillers consisting of lignocellulosic fillers (rice husk flour, beech bark flour) and mineral filler (nano-SiO_2).

In addition to extensive applications for solar cells [16], paints [17], etc., TiO_2 has been used in wood to improve the fire resistance [18], antifungal [19], and aging durability [20, 21] properties. Apart from their efficacy as thermal stabilizers [22, 23], their nanometric size makes them suitable for synergistic effects with organoclays, allowing combining both fire resistance performances and enhanced mechanical properties. The WPCs reinforced by nanoclay or metal oxides alone have been well documented [11, 24, 25]. However, to combine multiple natures of different nanoparticles into polymer matrix and hence further impregnation into wood has not been reported so far.

In this paper, the preparation WPNCs by vacuum impregnation of SAN, γ-methacryloyloxy trimethyl silane-modified TiO_2 nanoparticles in presence of nanoclay into simul wood has been presented. Our main objective was to evaluate the synergistic effect of the nanoparticles incorporation into wood on its physical properties like water repellency, dimensional stability, chemical resistance, thermal, and mechanical properties.

Experimental

Materials

Simul wood (*Bombax ceiba* L.) was collected locally. Styrene obtained from E. Merck (Mumbai, India), was purified by following standard procedure [26].

Acrylonitrile and 2,2′-azo bis isobutyronitrile (AIBN) were obtained from Merck (Germany) and used directly. TiO_2 nanopowder, <100 nm (BET) and γ-trimethoxy silyl propyl methacrylate (MSMA), nanoclay (nanomer, surface modified by 15–35 wt% octadecylamine and 0.5–5 wt% amino propyl triethoxy silane), were purchased from Sigma-Aldrich (USA). All other chemicals used were of analytical grade.

Sample preparation

The simul wood samples used for the study were prepared from clear defect-free wood, cut into blocks of 2.5 cm × 1 cm × 2.5 cm (radial × tangential × longitudinal) for dimensional stability, water uptake, chemical resistance, and hardness test.

Surface modification of nano-TiO_2

The surface of TiO_2 nanoparticles were modified by a silane coupling agent MSMA. The modification was done according to the method reported in the literature [27].

Preparation of styrene acrylonitrile copolymer

SAN was prepared in similar manner as described in our earlier communication [14].

Dispersion of SAN/TiO_2/nanoclay

Both the nanofillers, TiO_2 and nanoclay in appropriate amount were kept swelling in THF for 4 h in a round bottom flask under constant stirring followed by sonication for 15 min. The solution was then dispersed in SAN prepolymer and sonicated for another 15 min.

Preparation of Wood/SAN/TiO_2/nanoclay nanocomposite

Wood samples were preliminary dried in an oven at 105 °C until constant weight before treatment and dimensions and weight were measured. The samples were then placed in an impregnation chamber followed by application of load over each sample to prevent them from floatation during addition of prepolymer .Vacuum was applied for a specific time period for removing the air from the pores of the wood samples before addition of pre-polymeric mixture. Now the dispersion of SAN prepolymer–MSMA-modified TiO_2 nanopowder with nanoclay, and initiator, or dispersion of SAN prepolymer with MSMA-modified TiO_2 nanopowder and initiator, or that of SAN prepolymer and initiator was added from a dropping funnel to completely immerse the wood samples. The samples were then kept in the chamber at room temperature for another 4 h after attaining atmospheric pressure. This was the minimum time to get maximum polymer loading, which showed maximum improvement in properties. After impregnation, samples were taken out of the chamber and excess chemical were wiped from wood surfaces. The samples

were then wrapped in aluminum foil and cured at 90 °C for 24 h in an oven. This was followed by drying at 105 °C for another 24 h. The cured samples were then soxhlet extracted using chloroform to remove homo polymers, if any, formed during polymerization. Finally the samples were dried and the dimensions were measured by using slide caliper and weights were taken.

Measurements

FTIR study

The treated and untreated samples were grounded and Fourier transform infrared (FTIR) spectra were recorded by using a KBr pellet in a Nicolet (model Impact 410) FTIR spectrometer.

X-ray diffraction (XRD) studies

The XRD studies were done in a Rigaku X-ray diffractometer (Miniflex, UK) using Cu Kα radiation ($\lambda = 0.154$ nm) at a scanning rate of 1°/min from 2° to 70° of 2θ.

Thermogravimetric analysis

Thermal properties of the untreated and treated wood samples were measured by using a thermogravimetric analyzer, Shimadzu (model TA 50) at a heating rate of 10 °C/min up to 600 °C under nitrogen atmosphere.

Weight percent gain

Weight percent gain (WPG) after polymer loading was calculated according to formula

$$\text{WPG } (\%) = (W_2 - W_1)/W_1 \times 100$$

where W_1 is oven dry weight of wood blocks before polymer treatment and W_2 is oven dry weight of block after polymer treatment.

Volume increase (%) after impregnation

Percentage volume increase after curing of wood samples was calculated as follows:

$$\%\text{Volume increase} = (V_t - V_o)/V_o \times 100$$

where V_o is the oven dry volume of the untreated wood and V_t is the oven dry volume of the treated wood.

Hardness

The hardness of the samples was measured according to ASTM D 2240 method using a durometer (model RR12) and expressed as shore *D* hardness.

Water uptake and water vapor exclusion test

Both untreated and treated wood samples were immersed in distilled water at room temperature (30 °C) and weight was taken after different time intervals. It is expressed as

$$\text{Water uptake } (\%) = (W_t - W_d)/W_d \times 100$$

where W_t is the weight after immersion in distilled water for specific time period (0.5–168 h) and W_d is the weight of the oven dry sample.

For water vapor exclusion test, oven-dried samples were conditioned at 30 °C and 65 % relative humidity (RH) and weighed. Samples were then placed in a chamber where temperature and RH were maintained at 30 °C and 65 % RH, respectively. Weights were measured after different time periods (0.5–168 h). It is expressed as a percentage of moisture absorbed based on oven dry weight.

Dimensional stability test

Swelling in water

Dimensions of the oven-dried samples were measured and conditioned at room temperature (30 °C) and 30 % RH. Final placement of the samples was done in distilled water and then dimensions were remeasured after different time intervals.

In this case, swelling was considered as a change in volume and expressed as the percentage of volume increase compared to oven-dried samples.

$$\%\ \text{Swelling} = \left(V_{t,u} - V_o\right)/V_o \times 100$$

where $V_{t,u}$ is the volume of the treated or untreated wood after water absorption and V_o is the volume of treated or untreated wood before water absorption.

Antiswelling efficiency

The antiswell efficiency (ASE) index was determined to evaluate dimensional stability of treated wood specimens. The specimens were submerged in distilled water at 30 °C for different time periods after conditioning at 30 % RH and 30 °C. Volumetric swelling coefficients in percentage were calculated according to the formula:

$$S\,(\%) = (V_2 - V_1)/V_1 \times 100$$

where V_2 is the volume of the water-saturated wood blocks and V_1 is the volume of the oven-dried wood blocks. The values were obtained by measuring longitudinal,

tangential, and radial dimensions of the oven-dried and water-saturated blocks using slide caliper.

The percentage ASE was calculated from the wet and oven-dried volumes of treated and untreated wood specimens according to the formula below:

$$\text{ASE } (\%) = (S_c - S_t)/S_c \times 100$$

where S_c is the volumetric swelling coefficient of untreated blocks and S_t is the volumetric swelling coefficient of the treated wood blocks.

Chemical resistance test

The chemical resistance tests were evaluated by immersing the samples in 4 % NaOH solution and 4 % HCl solution for 24 h and 7 days. The percent of swelling was calculated by using the formula as given below:

$$\%\ \text{Swelling} = \left(V_{t,u} - V_o\right)/V_o \times 100$$

where $V_{t,u}$ is the volume of the untreated or treated wood after immersion in chemicals and V_o is the volume of the untreated and treated wood before immersion in chemicals.

Results and discussion

The optimum conditions for impregnation, at which maximum improvement in properties was observed, were as follows: vacuum: 508 mmHg, time of impregnation: 4 h, AIBN: 0.75 % (w/v), SAN (mL):100, THF (mL): 20, and modified TiO_2: 0.5–1.0 % (w/v). Nanoclay: 0.5–1.0 % (w/v).

Effect of variation of TiO_2/nanoclay on polymer loading (WPG %), volume increase and hardness

Related results are shown in Table 1. Polymer loading (%), volume increase (%) and hardness were found to enhance with the incorporation of either TiO_2, nanoclay or TiO_2/nanoclay into wood. The addition of TiO_2 alone improved all the properties. The higher the amount of TiO_2, the higher was the improvement. The improvement was further enhanced by the addition of nanoclay along with TiO_2.The improvement took place up to the addition of certain amount of nanoclay. Beyond that it deteriorated. The increase in both weight gain (%) and volume (%) was due to the filling of the void spaces in wood by polymer and nanoparticles. The overall improvement in hardness was due to the restriction in the mobility of polymer chain inside the clay interlayers. Besides this, the well-dispersed TiO_2 nanoparticles could act as filler which also reinforced the polymer matrix and increased hardness values. Hardness values were seen to decrease beyond the addition of 0.5 % each of TiO_2 and nanoclay. The agglomeration of clay layers at higher level of clay loading might be responsible for the decrease in the hardness value. The improvement of

Table 1 Effect of variation of TiO_2/nanoclay on polymer loading (WPG %) and volume increase and hardness

Sample particulars	Weight gain (%)[a]	Volume increase (%)[a]	Hardness (Shore *D*)[a]
Untreated	–	–	40 (±1.2)
Treated with SAN/THF/TiO_2/nanoclay			
100/20/0/0	34.17 (±1.4)	3.04 (±0.3)	42 (±0.9)
100/20/0.5/0	55.87 (±2.1)	4.12 (±0.2)	44 (±1.1)
100/20/1.0/0	115.15 (±1.9)	4.56 (±0.5)	56 (±1.4)
100/20/0/1.0	64.59 (±1.0)	4.45 (±0.8)	57 (±1.2)
100/20/0.5/0.5	168.03 (±0.4)	8.31 (±0.3)	67 (±1.9)
100/20/1.0/0.5	73.12 (±1.1)	6.05 (±0.9)	60 (±2.5)
100/20/0.5/1.0	124.70 (±2.3)	4.89 (±1.1)	58 (±1.1)

[a] Each value represents the average of five samples

properties in WPCs loaded with TiO_2 was more compared to that composite loaded with similar level of nanoclay. This might be due to the higher interaction between wood and polymer by modified TiO_2 compared to nanoclay.

FTIR studies

Figure 1 shows the FTIR spectra of (a) bare TiO_2, (b) MSMA, and (c) MSMA-modified TiO_2 nanoparticles. In the spectrum of bare TiO_2, the broad and sharp band at around 3,423 and 1,626 cm^{-1} for –OH stretching and –OH bending, respectively, were due to the adsorbed water on the surface of TiO_2 [28, 29]. For pure MSMA (curve b), the peaks at 2,831 and 2,945 cm^{-1} were assigned to the stretching vibration of C–H bonds. The peak at 1,719 cm^{-1} was assigned to the stretching vibration of the C=O. The peaks at 1,452 and 1,407 cm^{-1} were attributed to the methylene C–H bending vibration and vinyl C–H in plane bending vibration of MSMA. The two well-resolved peaks which appeared at around 1,322 and 1,300 cm^{-1} and the peak at 1,170 cm^{-1} were assigned to –C–CO–O– skeletal vibration originating from the methacryloxy group. The absorption band appeared at 1,626 cm^{-1} were for C=C double bond present in coupling agent. For MSMA-modified TiO_2, the absorption peaks characteristics of MSMA appeared in the spectrum of MSMA-modified TiO_2 (curve c) [30].The absorption band at 1,082 cm^{-1} reflected Si–O–Si structure that was produced by hydrolysis and polycondensation of the silane coupling agent. The results from FTIR indicated that the MSMA was grafted onto the surface of TiO_2 particles.

Figure 2 shows the FTIR spectra of (a) untreated wood, wood treated with (b) SAN, (c) SAN/TiO_2 (1.0 %), (d) SAN/nanoclay (1.0 %), (e) SAN/TiO_2 (0.5 %)/nanoclay (0.5 %), (f) SAN/TiO_2 (1.0 %)/nanoclay (0.5 %), and (g) SAN/TiO_2 (0.5 %)/nanoclay (1.0 %), respectively. The pure wood was characterized by the absorption bands (shown in curve 2a) appeared at 3,439 cm^{-1} (OH stretching), 1,740 cm^{-1} (C=O stretching of acetylated xylem) and 1,257 cm^{-1} (C–O stretching of acetyl groups), respectively. SAN treated wood (curve 2b) showed the absorption

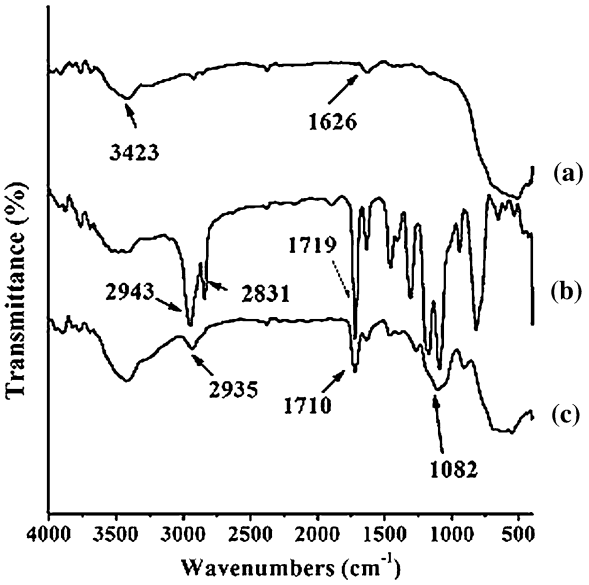

Fig. 1 FTIR spectra of (*a*) bare TiO_2, (*b*) MSMA, and (*c*) MSMA-modified TiO_2 nanoparticles

bands at 2,927 cm^{-1} (–CH_2 stretching), 2,242 cm^{-1} (C≡N stretching), and 762 cm^{-1} (aromatic C–H wagging) [31]. In the spectra of SAN-TiO_2 treated wood composites (curve 2c), the characteristic peaks for wood, SAN, and TiO_2 were observed. The peaks at 1456, 1253, and 1050 cm^{-1} were for Ti–O–C stretch vibrations [32], while the peak at 550 cm^{-1} was for Ti–O–Ti stretch vibration. The wide band observed in the frequency range of 800–500 cm^{-1} was the characteristic band of TiO_2 [33]. In the spectrum of SAN/nanoclay (1.0 %) (curve 2d), the presence of absorption bands at 532, 1040, and 3416 cm^{-1} originated from the nanoclay along with the characteristics peaks for SAN indicated the impregnation of SAN and nanoclay into wood. In the spectrum (curve 2e) of SAN/TiO_2 (0.5 %)/nanoclay (0.5 %) treated wood sample, all the characteristic absorption bands for MSMA-modified TiO_2 and nanoclay appeared. The intensity of the absorption band due to C–H methylene group was found to increase (curve 2f). However, The intensity of the band in the region 3,500–3,200 cm^{-1} was slightly decreased and shifted to lower wavenumbers, indicating a strong interaction between the hydroxyl groups of wood surface, nanoclay, and the impregnated TiO_2 nanoparticles through the hydrogen bond. This strong interaction led to the immobilization of TiO_2 nanoparticles in the wood matrix. The decrease in intensity of band and shifting of band to lower wave numbers for wood hydroxyl stretching frequency for the treatment with TiO_2 was reported in the literature [1]. In the spectrum of SAN/TiO_2 (0.5 %)/nanoclay (1.0 %) treated wood sample (curve 2g), the hydroxyl band shifted to lower intensity as well as there was a broadening of band. All these suggested a strong interaction between wood, SAN, nanoclay, and organically modified TiO_2 nanoparticles.

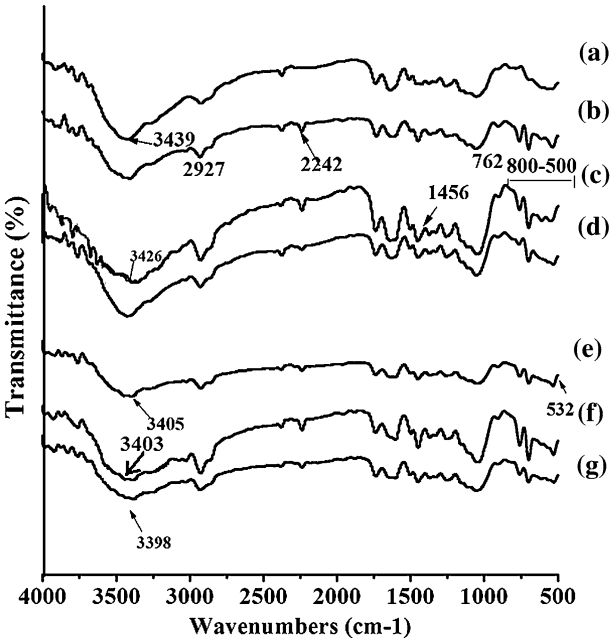

Fig. 2 FTIR spectra of (*a*) untreated wood and wood treated with (*b*) SAN, (*c*) SAN/TiO_2 (1.0 %), (*d*) SAN/nanoclay (1.0 %), (*e*) SAN/TiO_2 (0.5 %)/nanoclay (0.5 %), (*f*) SAN/TiO_2 (1.0 %)/nanoclay (0.5 %), and (*g*) SAN/TiO_2 (0.5 %)/nanoclay (1.0 %)

X-ray diffraction studies

Figure 3 represents the XRD spectra of (a) bare TiO_2 nanoparticles and (b) MSMA-modified TiO_2 nanoparticles. In the diffractogram of bare TiO_2 (curve a), the characteristics peaks appeared at $2\theta = 25.37°$ (101), 37.8° (004), 48.0° (200), 56.5° (211), 62.8° (204) for the anatase phase and 27.4° (110), 36.0° (101), 54.3° (105) for the rutile phase [34]. All peaks were in good agreement with the standard spectrum (JCPDS nos.: 88-1175 and 84-1286). The characteristics peaks for TiO_2 nanoparticles remained invariant after modification with MSMA, a silane coupling agent [35].

Figure 4 represents the X-ray diffractograms of (a) untreated wood, (b) nanoclay, and wood treated with (c) SAN, (d) SAN/nanoclay (1.0 %), (e) SAN/TiO_2 (1.0 %), (f) SAN/TiO_2 (0.5 %)/nanoclay (0.5 %), (g) SAN/TiO_2 (1.0 %)/nanoclay (0.5 %), and (h) SAN/TiO_2 (0.5 %)/nanoclay (1.0 %). It was observed that d (002) peak for the untreated wood at $2\theta = 22.3°$ was for the crystalline cellulose. The characteristic diffraction peak d (001) for nanoclay with basal spacing of $d = 2.152$ nm occurred at 4.1° (curve b). Curve c showing the diffractogram for SAN polymer exhibited a broad peak at $2\theta = 17.3°$ due to orthorhombic SAN (110) reflection. The diffractogram of wood sample treated with SAN/TiO_2 (1.0 %) was shown in curve d. The characteristic peaks for TiO_2 nanoparticles remained unchanged in the WPC which confirmed the impregnation of TiO_2 nanoprticles into wood. Curve e

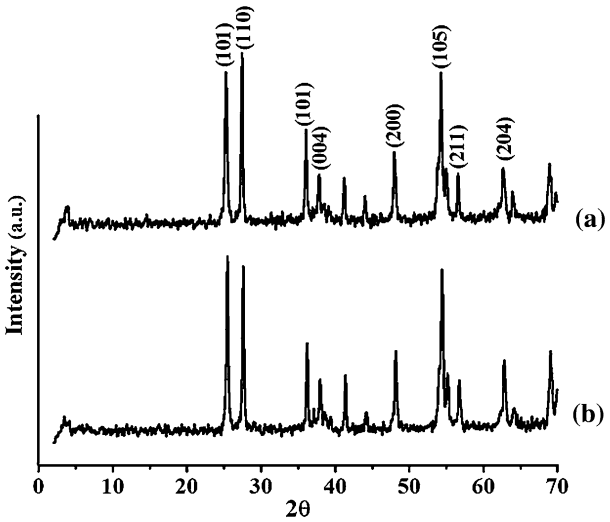

Fig. 3 X-ray diffraction spectra of (*a*) bare TiO_2 and (*b*) MSMA-modified TiO_2 nanoparticles

shows the diffractogram of SAN/nanoclay treated wood composite where a shifting of characteristic peak for wood to lower angle ($2\theta = 21.74°$) was occured. The corresponding peak for nanoclay at $2\theta = 4.1°$ disappeared. With the incorporation of nanoclay and SAN into wood, a shifting of crystalline peak of wood from higher to lower angle as well as disappearance of diffraction peak of nanoclay was observed. It could be said that either the full expansion of the clay gallery occurred, which was not possible to detect by XRD, or the clay layers became delaminated and no crystal diffraction peak appeared [14]. Curves f–h show the diffractograms for wood samples treated with SAN and different percentages of TiO_2/nanoclay. At lower level of loading of TiO_2, the characteristic peaks for TiO_2 were not detected and the diffraction peak for cellulose was also remained unchanged. However, the intensity for diffraction peak for cellulose in the composite increased and shifted to higher angle on increasing the TiO_2 amount. Some of the characteristic peaks of TiO_2 in the range $2\theta = 30°–70°$ were also found to appear. An increase in peak intensities of TiO_2 was reported by Mina et al. [36] during studying the XRD profile of polypropylene TiO_2 composite. No significant peak of TiO_2 was observed in wood samples loaded with higher percent of nanoclay along with TiO_2 nanoparticles. It could be concluded from these data that nanoclay layers were exfoliated and TiO_2 particles were dispersed in the WPC.

Thermogravimetric analysis

Figure 5 represents the thermogravimetric analysis of (a) bare TiO_2 nanoparticles and (b) MSMA-modified TiO_2 nanoparticles. A significant difference in thermal behavior was noticed. In the thermal degradation process, 8.23 and 12.24 % weight loss was observed for unmodified and modified nanoparticles, respectively.

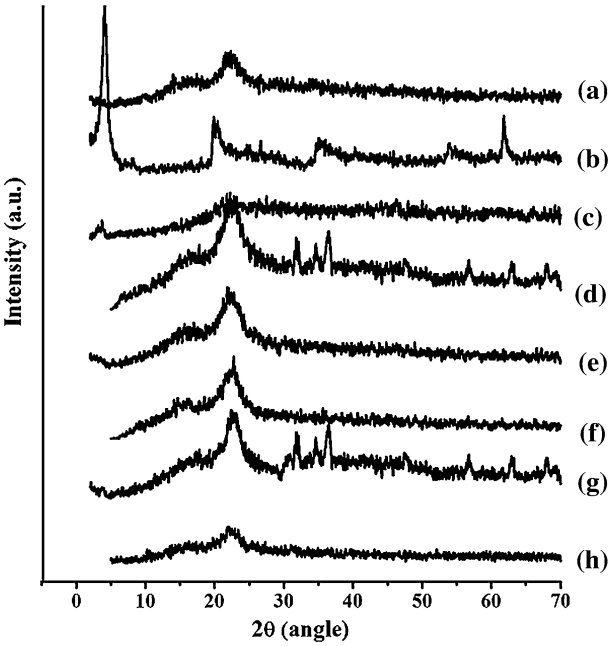

Fig. 4 X-ray diffraction spectra of (*a*) untreated wood, (*b*) nanoclay, and (*c*) SAN polymer, wood treated with (*d*) SAN/TiO_2 (1.0 %), (*e*) SAN/nanoclay (1.0 %), (*f*) SAN/TiO_2 (0.5 %)/ nanoclay (0.5 %), (*g*) SAN/TiO_2 (1.0 %)/nanoclay (0.5 %), and (*h*) SAN/TiO_2 (0.5 %)/nanoclay (1.0 %)

The higher weight loss was due to the decomposition of grafted MSMA from the surface of TiO_2. Table 2 shows the initial decomposition temperature (T_i), maximum pyrolysis temperature (T_m), temperature of decomposition (T_D) values at different weight losses for different samples, and residual weight (%) (RW) for untreated and polymer treated wood samples with or without TiO_2 and nanoclay. T_i value was highest for SAN/TiO_2 (0.5 %)/nanoclay (0.5 %) treated WPC. The T_m values of TiO_2 treated wood samples were more compared to those of wood samples treated with nanoclay. The highest T_m value was observed for wood treated with SAN/TiO_2 (0.5 %)/nanoclay (0.5 %) combination. RW (%) value of WPC treated with SAN/TiO_2/nanoclay (0.5:0.5) was found less compared to untreated wood but highest among the treated samples.

T_D values of polymer treated wood samples were observed higher than those of virgin wood samples. T_D values increased further on inclusion of silane modified TiO_2 and nanoclay either alone or in combination. T_D values were found maximum for the samples treated with SAN/TiO_2 (0.5 %)/nanoclay (0.5 %) combination. But beyond that it decreased. The higher T_D values might be due to the combining effect of crosslinked structure formed by MSMA present in TiO_2 and the presence of silicate layers. The crosslinked structure reduced the rate of decomposition of degradable components in the WPNC. Similar findings were reported by Devi and Maji [37]. The presence of silicate layer acted as a barrier and hindered the diffusion of volatile decomposition products. Moreover, higher thermal diffusivity of TiO_2

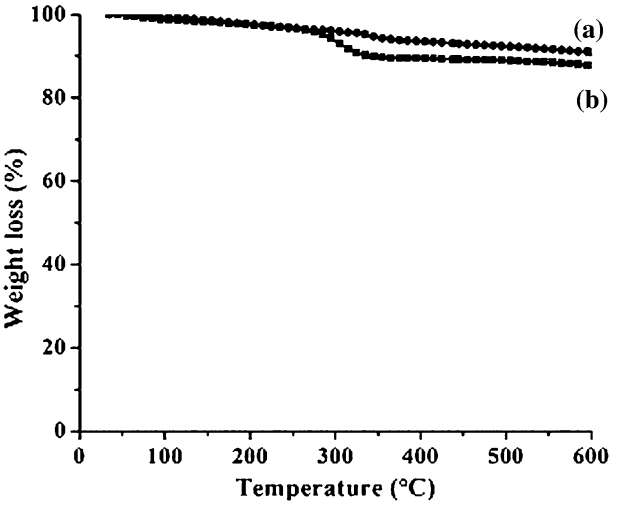

Fig. 5 TGA of (*a*) bare TiO_2 and (*b*) MSMA-modified TiO_2 nanoparticles

Table 2 Thermal analysis of untreated and treated wood

Sample particulars	T_i	T_m [a]	T_m [b]	Temperature of decomposition (T_D) in °C at different weight loss (%)				RW (%) at 500 °C
				20	40	60	80	
Untreated wood	225	235	341	275	303	336	–	23.8
Wood treated with SAN/TiO_2/nanoclay								
100/0/0	242	325	379	277	302	349	430	8.19
100/1.0/0	247	359	391	290	328	381	407	4.75
100/0/1.0	244	321	395	287	318	369	446	12.3
100/0.5/0.5	252	363	410	300	343	392	433	14.7
100/1.0/0.5	250	360	408	296	335	388	416	11.8
100/0.5/1.0	246	346	398	293	330	382	413	12.7

T_i value for initial degradation

[a] T_m value for 1st step, [b] T_m value for 2nd step

nanoparticles provided a better dispersion of heat inside the composite resulting in delay of burning of surface and hence release of combustible volatiles throughout the composites. A significant increase in thermal stability of PMMA due to synergistic effect of clay and TiO_2 was reported by Laachachi et al. [23] while studying the thermal stability of PMMA by using organoclay and TiO_2. The clay and TiO_2 nanoparticles might exist in the agglomerated form at higher percentage of loading and offered an easy way to the passage of volatile products. Hence, the thermal stability decreased at higher level of loading of nanoparticle.

Water uptake and water vapor exclusion study

Water uptake capacity for untreated wood and treated wood is shown in Fig. 6. From the figure, it was observed that the water uptake (%) was maximum for the untreated wood samples. With the increase in time, the capillaries and void spaces were getting sufficient time to become filled up with water which resulted in an increase in the water uptake capacity. In treated samples, the void spaces decreased due to filling of the same by SAN copolymer. Water absorption decreased on further incorporation of either TiO_2 or nanoclay. Wood samples treated with SAN/TiO_2 (0.5 %)/nanoclay (0.5 %) showed lowest water uptake followed by SAN/TiO_2 (0.5 %)/nanoclay (1.0 %) and SAN/TiO_2 (1.0 %)/nanoclay (0.5 %) throughout the studied time period. The silicate layers of the clay generated the tortuous pathway and increased the barrier property for diffusion of water within the nanocomposites. Similar results were also cited in the literature [11]. TiO_2 nanopowder also provided a barrier to the passage of water. The better the distribution of nanoparticles, the better was the barrier property. At a fixed percentage of nanoclay, water uptake increased with the increase in the percentage of TiO_2 in TiO_2/nanoclay combination. This was due to the strong affinity of water molecules towards TiO_2 particles that restricted its free motion. The well distribution nature of modified TiO_2 nanoparticles further improved the resistance and retarded the diffusion of water molecules throughout the composites. The improvement in water and dimensional stability for wood through TiO_2 coating was reported by Sun et al. [1]. The observed higher water uptake at higher clay loading was due to the agglomeration of clay layers.

Water vapor exclusion test was carried out at 30 °C and 65 % RH for untreated and treated wood and is shown in Fig. 7. Moisture uptake was found to increase

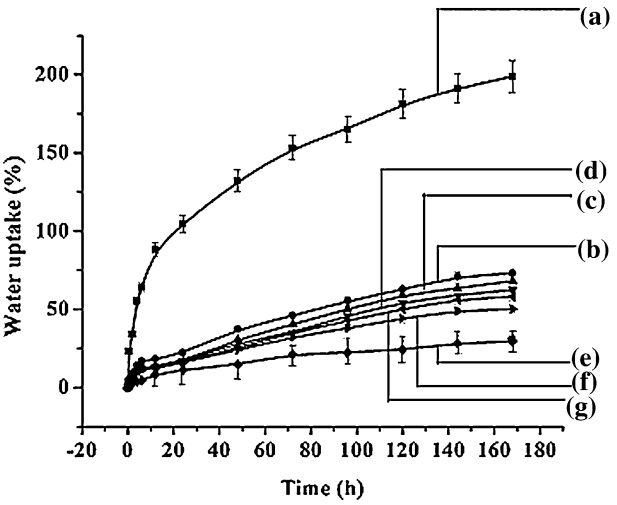

Fig. 6 Water uptake (%) as a function of time of (*a*) untreated wood and wood treated with (*b*) SAN, (*c*) SAN/TiO_2 (1.0 %), (*d*) SAN/nanoclay (1.0 %), (*e*) SAN/TiO_2 (0.5 %)/nanoclay (0.5 %), (*f*) SAN/TiO_2 (1.0 %)/nanoclay (0.5 %), and (*g*) SAN/TiO_2 (0.5 %)/nanoclay (1.0 %)

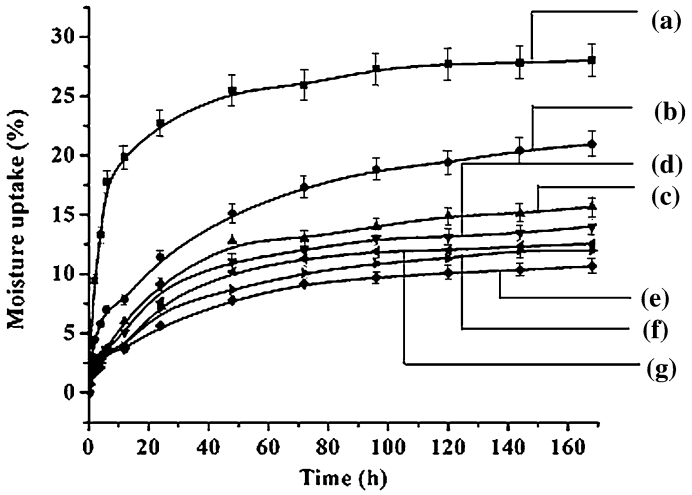

Fig. 7 Moisture uptake (%) as a function of time of (*a*) untreated wood and wood treated with (*b*) SAN, (*c*) SAN/TiO_2 (1.0 %), (*d*) SAN/nanoclay (1.0 %), (*e*) SAN/TiO_2 (0.5 %)/ nanoclay (0.5 %), (*f*) SAN/TiO_2 (1.0 %)/nanoclay (0.5 %), and (*g*) SAN/TiO_2 (0.5 %)/nanoclay (1.0 %)

with time. Hydrophilic nature of untreated wood was responsible for showing highest water uptake. Impregnation of wood with SAN copolymer would fill the void spaces and capillaries present in the wood. The presence of MSMA on the surface of TiO_2 would form the crosslinking between TiO_2 nanoparticles, wood and polymer due to which it absorbed less water. Water diffusivity further decreased on addition of clay due to increase in tortuous path as explained earlier. The trend and explanation for water vapor uptake of different samples were similar to those of samples taken for water uptake study.

Dimensional stability test

The results showing the effect of swelling in water vapor for untreated and treated wood samples at room temperature (30 °C) for different time periods are shown in Fig. 8. As expected, wood treated with SAN and TiO_2 (0.5 %)/nanoclay (0.5 %) showed least swelling. This was due to the uniform distribution of TiO_2 nanoparticles and increase in silicate layer spacing caused by the presence of organic modifier in nanoclay along with the deposition of crosslinked SAN polymer in the void spaces of wood.

Antiswelling efficiency

The results of antiswelling efficiency of wood samples are shown in Table 3. Antiswelling efficiency was found to increase with the increase of time. The antiswelling efficiency was more in the case of WPNC. The improvement in dimensional stability of wood composites over virgin wood samples might be due to the deposition of polymer in void spaces of the wood composites. As the polymer

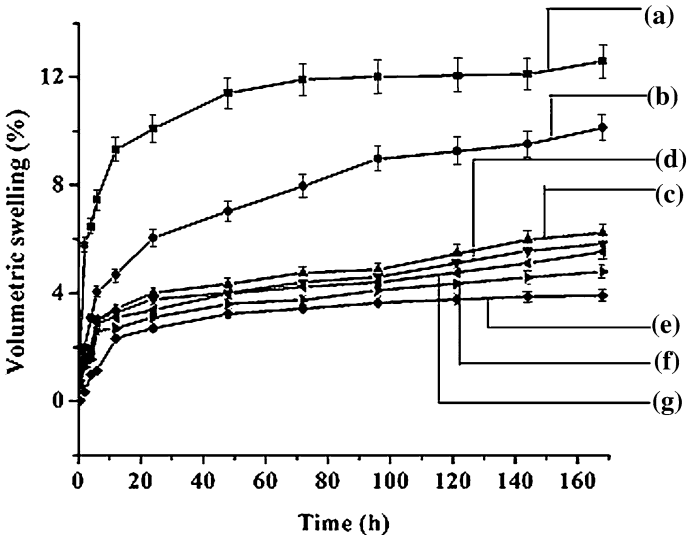

Fig. 8 Volumetric swelling as a function of time of (*a*) untreated wood and wood treated with (*b*) SAN, (*c*) SAN/TiO_2 (1.0 %), (*d*) SAN/nanoclay (1.0 %), (*e*) SAN/TiO_2 (0.5 %)/nanoclay (0.5 %), (*f*) SAN/TiO_2 (1.0 %)/nanoclay (0.5 %), and (*g*) SAN/TiO_2 (0.5 %)/nanoclay (1.0 %)

Table 3 Antiswell efficiencies of treated wood

Time (h)	SAN	SAN/TiO_2 (1.0 %)	SAN/ nanoclay (1.0 %)	SAN/TiO_2 (0.5 %)/ nanoclay (0.5 %)	SAN/TiO_2 (1.0 %)/ nanoclay (0.5 %)	SAN/TiO_2 (0.5 %)/ nanoclay (1.0 %)
0.5	46.44 (±1.2)	58.46 (±1.6)	61.74 (±7.4)	97.81 (±3.4)	66.12 (±3.6)	69.39 (±3.9)
2	65.28 (±2.1)	71.50 (±2.1)	73.05 (±3.4)	94.12 (±2.4)	74.95 (±3.5)	78.23 (±3.1)
4	52.03 (±3.1)	70.80 (±3.4)	69.25 (±3.4)	84.78 (±1.4)	72.36 (±2.8)	76.08 (±3.0)
6	45.84 (±1.2)	59.65 (±2.6)	59.78 (±4.4)	84.85 (±0.9)	60.85 (±1.9)	65.14 (±1.8)
12	49.83 (±1.1)	63.26 (±1.7)	64.76 (±1.9)	74.97 (±1.5)	66.70 (±2.2)	70.99 (±1.4)
24	40.07 (±1.3)	60.21 (±1.5)	62.5 (±1.1)	73.21 (±2.1)	66.56 (±3.4)	69.24 (±1.2)
48	38.33 (±1.8)	61.92 (±1.4)	64.91 (±1.7)	71.66 (±1.8)	65.08 (±1.0)	68.42 (±1.7)
72	33.16 (±1.9)	60.11 (±1.3)	62.97 (±2.7)	71.28 (±1.6)	64.39 (±0.9)	68.51 (±1.6)
96	25.31 (±3.2)	59.45 (±1.2)	61.69 (±2.6)	69.6 (±1.1)	63.36 (±2.5)	65.86 (±1.6)
120	21.38 (±4.4)	50.61 (±1.5)	54.08 (±2.8)	68.04 (±2.9)	57.88 (±1.8)	62.18 (±1.4)
144	15.94 (±3.4)	48.25 (±2.4)	51.66 (±3.1)	67.52 (±2.6)	54.06 (±3.1)	60.21 (±0.7)
168	26.47 (±2.0)	45.23 (±0.9)	50.98 (±3.4)	67.12 (±1.7)	53.45 (±2.7)	59.02 (±0.7)

Each value represents the average of five samples

was less hygroscopic than wood, less water would be absorbed during humid conditions. MSMA-modified TiO_2 treatment remarkably improved the ASE of the treated wood. MSMA-modified TiO_2 might get deposited into the void spaces of wood to make the cell wall more bulky. As a result, shrinking and swelling would be

Table 4 Chemical resistance test for untreated and treated wood samples

Medium	Duration (h)	Volumetric swelling (%)						
		Untreated wood	Wood treated with					
			SAN	SAN/TiO_2 (1.0 %)	SAN/nanoclay (1.0 %)	SAN/TiO_2 (0.5 %)/ nanoclay (0.5 %)	SAN/TiO_2 (1.0 %)/ nanoclay (0.5 %)	SAN/TiO_2 (0.5 %)/ nanoclay (1.0 %)
4 % NaOH	24	10.09 (±0.9)	5.09 (±0.4)	3.14 (±0.3)	3.22 (±0.6)	1.59 (±0.1)	2.43 (±0.1)	2.55 (±0.5)
	168	11.10 (±0.7)	6.86 (±0.5)	4.58 (±0.7)	4.96 (±0.8)	3.78 (±0.4)	3.98 (±0.7)	4.03 (±0.3)
4 % HCl	24	6.14 (±0.8)	3.45 (±0.4)	1.69 (±0.3)	2.32 (±0.6)	1.12 (±0.5)	1.34 (±0.1)	1.45 (±0.8)
	168	9.13 (±1.4)	5.76 (±0.9)	3.12 (±0.3)	3.32 (±0.5)	2.76 (±0.3)	2.98 (±0.5)	3.08 (±0.7)

Each value represents the average of five samples

reduced and hence dimensional stability would be improved. The dimensional stability was further improved by the addition of organically modified nanoclay. The improvement was highest for TiO_2 (0.5 %)/nanoclay (0.5 %) followed by TiO_2 (0.5 %)/nanoclay (1.0 %) by TiO_2 (1.0 %)/nanoclay (0.5 %). At similar level of loading, ASE for wood samples treated with nanoclay (1.0 %) was higher than that of wood sample treated with TiO_2. The increase in ASE of scots pine for the treatment with different types of organo alkoxy silane was also reported [38].

Chemical resistance test

Related results are shown in Table 4. It was observed that treated wood samples swelled less compared to untreated samples. The swelling was least in the case of TiO_2/nanoclay (0.5:0.5) treated wood /SAN composite. The cell wall of the wood only thickened due to incorporation of SAN. MSMA present in TiO_2 nanoparticles formed a network structure between wood, TiO_2 nanoparticles, and SAN polymer and as a result swelling decreased. The inclusion of clay further increased the tortuous pathway for the diffusion of chemicals which in turn would decrease the swelling. In all the cases, the swelling was less in hydrochloric acid compared to sodium hydroxide solution. This may be possibly due to the increase in interaction by sodium hydroxide with wood cellulose and clay layers [14].

Conclusions

Surface modification of TiO_2 nanoparticles with γ-methacryloyloxy trimethyl silane (MSMA) was successfully done and characterized by FTIR, XRD, and thermogravimetry (TGA) analysis. The interaction between wood, SAN, nanoclay, and organically modified TiO_2 nanoparticles were investigated by FTIR. The exfoliation of nanoclay and dispersion of TiO_2 were studied by XRD. Highest thermal stability was achieved for the wood sample treated with SAN/TiO_2 (0.5 %)/nanoclay (0.5 %) as revealed by TGA. With the incorporation of MSMA-modified TiO_2 nanoparticles and nanoclay in the ratio of (0.5:0.5) into wood/SAN polymer matrix, water resistance, dimensional stability, and chemical resistance were found to improve.

References

1. Sun Q, Lu Y, Liu Y (2011) Growth of hydrophobic TiO_2 on wood surface using a hydrothermal method. J Mater Sci 46:7706–7712
2. Rowell RM (2005) Handbook of wood chemistry & wood composites. CRC Press, Washington, DC
3. Kumar S (1994) Chemical modification of wood. Wood Fiber Sci 26:270–280
4. Bryne LE, Walinder MEP (2010) Ageing of modified wood. Part 1: wetting properties of acetylated, furfurylated, and thermally modified wood. Holzforschung 64(3):295–304
5. Thygesen LG, Engelund ET, Hoffmeyer P (2010) Water sorption in wood and modified wood at high values of relative humidity. Part I: results for untreated, acetylated, and furfurylated Norway spruce. Holzforschung 64(3):315–323

6. Li Y, Wu Q, Li J, Liu Y, Wang XM, Liu Z (2012) Improvement of dimensional stability of wood via combination treatment: swelling with maleic anhydride and grafting with glycidyl methacrylate and methyl methacrylate. Holzforschung 66(1):59–66
7. Xiao Y, Xie Z, Mai C (2012) The fungal resistance of wood modified with glutaraldehyde. Holzforschung 66(2): 237–243
8. Ziaei Tabari H, Nourbakhsh A, Ashori A (2011) Effects of nanoclay and coupling agent on the mechanical, morphological, and thermal properties of wood flour/polypropylene composites. Polym Eng Sci 51(2):272–277
9. Sheshmani S, Ashori A, Hamzeh Y (2010) Physical properties of polyethylene/woodfiber/organoclay nanocomposites. Appl Polym Sci 118(6):3255–3259
10. Kiani H, Ashori A, Mozaffari SA (2011) Water resistance and thermal stability of hybrid lignocellulosic filler–PVC composites. Polym Bull 66(6):797–802
11. Cai X, Riedl B, Zhang SY, Wan H (2008) The impact of nature of nanofillers on the performance of wood polymer nanocomposites. Compos A 39:727–737
12. Zhao G, Lu WH (2008) Structure and characterization of Chinese fir (*Cunninghamia lanceolata*) wood/MMT intercalation nanocomposite (WMNC). Front For China 3(1):121–126
13. Devi RR, Maji TK (2012) Chemical modification of simul wood with styrene–acrylonitrile copolymer and organically modified nanoclay. Wood Sci Technol 46:299–315
14. Devi RR, Maji TK (2011) Physical properties of simul (red-silk cotton)-wood (*Bombax ceiba* L.) chemically modified with styrene-acrylonitrile co-polymer and nanoclay. Holzforschung. doi: 10.1515/hf.2011.164
15. Nourbakhsh A, Farhani Baghlani F, Ashori A (2011) Nano-SiO_2 filled rice husk/polypropylene composites: physico-mechanical properties. Ind Crops Prod 33(1):183–187
16. O'regan B, Gratzel M (1991) A low-cost, high-efficiency solar cell based on dye sensitized colloidal TiO_2 films. Nature 353:737–740
17. Kim T, Lee M, Lee S, Park Y, Jung C, Boo J (2005) Development of surface coating technology of TiO_2 powder and improvement of photocatalytic activity by surface modification. Thin Solid Films 475:171–177
18. Miyafuji H, Saka S (1997) Fire-resisting properties in several TiO_2 wood–inorganic composites and their topochemistry. Wood Sci Technol 31:449–455
19. Chen F, Yang X, Wu Q (2009) Antifungal capability of TiO_2 coated film on most wood. Build Environ 44:1088–1093
20. Mahltig B, Swaboda C, Roessler A, Bottcher H (2008) Functionalising wood by nanosol application. J Mater Chem 18:3180–3192
21. Schmalzl KJ, Evans PD (2003) Wood surface protection with some titanium, zirconium and manganese compounds. Polym Degrad Stab 82:409–419
22. Kuljanin J, Marinovic-Cincovic M, Zec S, Comor MI, Nedeljkovic JM (2003) Influence of Fe_2O_3-filler on the thermal properties of polystyrene. J Mater Sci Lett 22(3):235–237
23. Laachachi A, Cochez M, Ferriol M, Leroy E, Lopez-Cuesta JM (2005) Influence of TiO_2 and Fe_2O_3 fillers on the thermal properties of poly(methyl methacrylate) (PMMA). Mater Lett 59:36–39
24. Clausen CA, Kartal SN, Arango RA, Green F (2011) The role of particle size of particulate nano-zinc oxide wood preservatives on termite mortality and leach resistance. Nanoscale Res Lett 6:427
25. Jinshu S, Jianzhang L, Wenrui Z, Derong Z (2007) Improvement of wood properties by urea–formaldehyde resin and nano-SiO_2. Front For China 2(1):104–109
26. Ashraf SM, Ahmad S, Riaz U (2009) A laboratory manual of polymers. Volume 1. Experiments in material science and material chemistry. I K International Pvt Ltd, New Delhi
27. Rong Y, Chen HZ, Wu G, Wang M (2005) Preparation and characterization of titanium dioxide nanoparticle/polystyrene composites via radical polymerization. Mater Chem Phys 91:370–374
28. Deng C, James PF, Wright PV (1998) Poly(tetraethylene glycol malonate)–titanium oxide hybrid materials by sol–gel methods. J Mater Chem 8:153–159
29. Park HK, Kim DK, Hee DJ (1997) Effect of solvent on Titania particle formation and morphology in thermal hydrolysis of $TiCl_4$. J Am Ceram Soc 80:743–749
30. Siddiquey IA, Ukaji E, Furusawa T, Sato M, Suzuki N (2007) Preparation and characterization of titanium dioxide nanoparticle/polystyrene composites via radical polymerization. Mater Chem Phys 105:162–168
31. Yap MGS, Que YT, Chia LH (1991) FTIR characterization of tropical wood-polymer composites. J Appl Polym Sci 43:2087–2090

32. Colomer MT, Velasco MJ (2007) Rutile-type dense ceramics fabricated by pressureless sintering of $Ti_{1-x}Ru_xO_2$ powders prepared by sol–gel. J Eur Ceram Soc 27:2369–2376
33. Fujishima A, Rao TN, Tryk DA (2000) Titanium dioxide photocatalysis. J Photobiol Photochem Rev 1:1–21
34. Thamaphat K, Limsuwan P, Ngotawornchai B (2008) Phase characterization of TiO_2 powder by XRD and TEM. Kasetsart J (Nat Sci) 42:357–361
35. Deng K, Ren X, Jiao Y, Tian H, Zhang P, Zhong H, Liu Y (2010) Preparation of poly(methyl acrylate)/TiO_2 composites by potassium diperiodato cuprate initiated grafting copolymerization. Iran Polym J 19(1):17–25
36. Mina F, Seema S, Matin R, Rahaman J, Sarker RB, Gafur A, Bhuiyan AH (2009) Improved performance of isotactic polypropylene/titanium dioxide composites: effect of processing conditions and filler content. Polym Degrad Stab 94(2):183–188
37. Devi RR, Maji TK (2007) Effect of glycidyl methacrylate on the physical properties of wood–polymer composites. Polym Compos 28:1–5
38. Panov D, Terziev N (2009) Study on some alkoxysilanes used for hydrophobation and protection of wood against decay. Int Biodeterior Biodegrad 63(4):456–461